

Supporting Information

Effective advance treatment of secondary effluent from industrial parks by the Mn-based catalyst catalytic ozonation process

Zhijuan Niu ^{1,2}, Shihao Han ¹, Weihua Qin ³, Pan Gao ⁴, Feng Xiao ¹, Shaoxia Yang ^{1,*}

1 School of Water Resources and Hydropower Engineering, North China Electric Power University, Beijing 102206, China

2 Research Center for Eco-Environmental Engineering, Dongguan University of Technology, Dongguan 523808, China

3 CCCC Highway Consultants Co. Ltd., Beijing 100010, China

4 National Engineering Laboratory for Biomass Power Generation Equipment, School of Renewable Energy, North China Electric Power University, Beijing 102206, China

Corresponding author:

Dr. Shaoxia Yang

Tel: +8610 61772456

Fax: +8610 61772230

E-mail: yangshaoxia@ncepu.edu.cn (S.X. Yang)

Text Captions

- Text S1** Analytical method of COD.
Text S2 The detailed calculating course and key parameter definition of FRI method.
Text S3 The definition of some indicators.
Text S4 Contributions of ROS and O₃ oxidation in the Mn-based catalyst/O₃ system.

Table Captions

- Table S1** The characteristics of secondary effluent from IPWWTPs.
Table S2 Five fluorescence integral regions.
Table S3 FRI parameters for operationally defined 3D-EEM regions and volumetric (Φ) and removal rate for 3D-EEM analysis of water samples collected in ozonation alone process and catalytic ozonation process.
Table S4 Elemental composition of the Mn-based catalyst.

Figure Captions

- Fig. S1** Simplified diagram of the catalytic ozonation device.
Fig. S2 Influence of ozone dosage on the TOC removal in secondary effluent from IPWWTPs in the ozonation alone process (pH = 4.0, $t = 25$ °C).
Fig. S3 Influence of ozone dosage on the initial reaction rate (k) for COD removal in secondary effluent from IPWWTPs in the ozonation alone process (pH = 4.0, $t = 25$ °C).
Fig. S4 Influence of ozone dosage on TN removal in secondary effluent from IPWWTPs in the ozonation process (a). (pH = 4.0, $t = 25$ °C). Influence of different catalyst on TN removal in secondary effluent from IPWWTPs in the catalytic ozonation process (b). ($[O_3] = 0.84$ g/h, $[Catalyst] = 100$ g/L, pH = 4.0, $t = 25$ °C).
Fig. S5 Impacts of ozone dosage on the COD removal (a) and ozone utilization efficiency (b) in the Mn-based catalytic ozonation process. ($[Catalyst] = 100$ g/L, pH = 4.0, $t = 25$ °C).
Fig. S6 Impacts of operating conditions on the TOC removal in secondary effluent from IPWWTPs in the Mn-based catalytic ozonation process. Ozone dosage (a). ($[Catalyst] = 100$ g/L, pH = 4.0, $t = 25$ °C). Catalyst dosage (b). ($[O_3] = 0.84$ g/h, pH = 4.0, $t = 25$ °C). pH value (c). ($[O_3] = 0.84$ g/h, $[Catalyst] = 100$ g/L, $t = 25$ °C). Catalyst cycle times (d). ($[O_3] = 0.84$ g/h, $[Catalyst] = 100$ g/L, pH = 4.0, $t = 25$ °C).
Fig. S7 FOMs removal speed during the ozonation reaction. Ozonation alone process. ($[O_3] = 0.84$ g/h, pH = 4.0, $t = 25$ °C). Catalytic ozonation process. ($[O_3] = 0.84$ g/h, $[Catalyst] = 100$ g/L, pH = 4.0, $t = 25$ °C).
Fig. S8 N₂ adsorption-desorption isotherms (a) and pore distribution (b) of Mn-based catalyst.
Fig. S9 XRD patterns of Mn-based catalyst.
Fig. S10 FTIR spectra of the fresh and used Mn-based catalysts.

1 **Text S1** Analytical method of COD.

2 (1) Masking agent

3 Taking 10.0 g of analytically pure mercury sulfate dissolved in 100 mL of 10% sulfuric acid
4 and then mixed evenly.

5 (2) Digestion solution

6 Taking 2.45 g of potassium dichromate, 50.0 g of potassium aluminum sulfate and 10.0 g of
7 ammonium molybdate dissolved in 500 mL deionized water, and then add 200mL concentrated
8 sulfuric acid, after cooling, constant volume in 1000mL volumetric flask, and mixed evenly.

9 (3) Catalyst liquid

10 Taking 8.8g of analytically pure silver sulfate dissolved in 1000mL of concentrated sulfuric
11 acid and then mixed evenly.

12 (4) Detection of COD in secondary effluent from IPWWTPs

13 2.5 mL of water sample was taken into the digestion tube, and 0.5 mL of masking agent, 1 mL
14 of digestive solution and 3.5 mL of catalytic solution were added in turn. The digestion was carried
15 out at 165 °C for 15 min in the digestion instrument, and the solution was taken out and reduced to
16 room temperature. Then placed in a centrifuge tube, centrifuged at 8000 r/min for 15 min ; the
17 absorbance A was measured at 446 nm by spectrophotometer. And then the corrected absorbance
18 A_{abs} ($A_{\text{abs}} = A - A_0$) was obtained, and the concentration of COD in the water sample to be
19 measured was obtained from the standard curve.

20

21 **Text S2** The detailed calculating course and key parameter definition of FRI method.

22 Fluorescence regional integration (FRI) method was used to quantify the organic pollutant in
23 fluorescence regions of 3D-EEM spectroscopy. The fluorescence regions was divide into five parts,
24 including aromatic protein I in region 1(R1), aromatic protein II in region 2 (R2), fulvic acid in
25 region 3 (R3), soluble microbial products in region 4 (R4) and humic acids in region 5 (R5), the
26 detailed result was shown in Table S2. Firstly, the integral volume (Φ_i) of specific fluorescence
27 region was calculated by integral method; secondly, the integration standard volume ($\Phi_{i,n}$) of
28 specific fluorescence regions was obtained by the standardization of Φ_i , which could characterize
29 the relative content of specific structure organic matter in the specific fluorescence region. The
30 relevant formulas were shown in Eqs. (1)-(3) (Chen et al., 2003):

$$31 \quad \Phi_{i,n} = MF_i \Phi_i = MF_i \int_{E_x} \int_{E_m} I(\lambda_{E_x}, \lambda_{E_m}) d_{E_x} d_{E_m} \quad (1)$$

$$32 \quad \Phi_{T,n} = \sum_{i=1}^5 \Phi_{i,n} \quad (2)$$

$$33 \quad P_{i,n} = \frac{\Phi_{i,n}}{\Phi_{T,n}} \times 100\% \quad (3)$$

34 Where, $\Phi_{i,n}$ is the integral standard volume of fluorescence region i , $\text{AU} \cdot \text{nm}^2$; Φ_i is the integral
35 volume of fluorescence region i , $\text{AU} \cdot \text{nm}^2$; λ_{E_x} is the excitation wavelength, nm; λ_{E_m} is the
36 emission wavelength, nm; $I(\lambda_{E_x}, \lambda_{E_m})$ is the Fluorescence intensity corresponding to
37 excitation-emission wavelength, AU; $\Phi_{T,n}$ is the total integral standard volume of fluorescence
38 region, $\text{AU} \cdot \text{nm}^2$; $P_{i,n}$ is the proportion of integral standard volume of fluorescence region i to total
39 integral standard volume, %; MF_i is the multiplication factor, which is the reciprocal of the
40 integral area of the fluorescent region i to the total area of the fluorescent region.

41

42 **Text S3** The definition of some indicators.

43 The ozone utilization efficiency (OUE), expressed as the COD removal per unit of ozone
44 dosage of ozone per minute, calculated in this work as follows Eqs. (4):

$$45 \quad OUE = \frac{COD_{in} - COD_{out}}{(Ozone\ dosage) \cdot t} \quad (4)$$

46 Where COD_{in} and COD_{out} represent the COD concentration in the influent and effluent, respectively;

47 t represents the sampling time.

48 The pseudo-first-order kinetic model was applied to calculate the initial reaction rate for
49 catalytic ozonation of COD, and expressed by following Eq. (5) (Peng et al., 2022):

$$50 \quad \ln\left(\frac{C_t}{C_0}\right) = -k \cdot t \quad (5)$$

51 Where C_t is the concentration of COD at instant t , C_0 is the initial COD concentration, k represents
52 the kinetic rate constant, and t is the reaction time.

53 **Text S4.** Contributions of ROS and O₃ oxidation in the Mn-based catalyst/O₃ system.

54 Based on the k value of COD removal in ozonation alone system (0.0064 min⁻¹) and catalytic
55 ozonation over Mn-based catalyst system (0.0731 min⁻¹), the relative contributions of ROS and O₃
56 to COD removal in the Mn-based catalyst/O₃ system were determined as follows (Yao et al., 2021):

$$57 \quad \eta_{O_3} = \frac{k_{\text{Ozonation alone}}}{k_{\text{Catalytic ozonation}}} \times 100\% = \frac{0.0064 \text{ min}^{-1}}{0.0731 \text{ min}^{-1}} \times 100\% = 8.8\% \quad (6)$$

$$58 \quad \eta_{ROS} = 100\% - \eta_{O_3} = 100\% - 8.76\% = 91.2\% \quad (7)$$

59 Where η_{O_3} stands for the contribution of direct oxidation; η_{ROS} stands for the contribution of ROS
60 oxidation; $k_{\text{Ozonation alone}}$ stands for the k value of COD removal in ozonation alone system; $k_{\text{Catalytic}}$
61 ozonation stands for the k value of COD removal in catalytic ozonation over Mn-based catalyst system.
62

Table S1 The characteristics of secondary effluent from IPWWTPs.

Parameters	Value (mean \pm s.d.)
COD (mg/L)	78.3 \pm 2.1
TOC (mg/L)	27.0 \pm 1.2
TN (mg/L)	11.2 \pm 3.2
UV ₂₅₄ (cm ⁻¹)	0.725 \pm 0.032
NO ₃ ⁻ (mg/L)	25.3 \pm 0.5
Cl ⁻ (mg/L)	1 600.0 \pm 15.0
SO ₄ ²⁻ (mg/L)	429.7 \pm 5.4
Initial pH	4.0 \pm 0.1

Table S2 Five fluorescence integral regions.

EEM region	Organic pollutant type	Ex/nm	Em/nm
R1	aromatic protein I	200-250	280-330
R2	aromatic protein II	200-250	330-380
R3	fulvic acid	200-250	380-550
R4	soluble microbial products	250-280	280-380
R5	humic acids	250-400	380-550

67 **Table S3** FRI parameters for operationally defined 3D-EEM regions and volumetric (Φ) and removal rate for 3D-EEM analysis of water samples
 68 collected in ozonation alone process and the catalytic ozonation process.

EEM region	FRI parameters			$\Phi_{i,n}$ ($\times 10^7$ AU \cdot nm 2)							Removal rate (%)					
	PA ^a (nm 2)	FPA ^b (nm 2)	MF _i	Raw	O-20	O-40	O-60	CO-20	CO-40	CO-60	O-20	O-40	O-60	CO-20	CO-40	CO-60
R1	2500	0.060	16.7	9.4	3.8	2.5	2.3	0.2	1.8	0.8	59.6	73.4	75.5	97.9	80.9	91.5
R2	2500	0.060	16.7	8.9	3.7	2.8	2.7	1.8	2.2	1.3	58.4	68.5	69.7	79.8	75.3	85.4
R3	8500	0.202	5.0	4.9	1.8	1.4	1.2	0.7	0.5	0.5	63.3	71.4	75.5	85.7	89.8	89.8
R4	3000	0.071	14.1	12.0	4.2	3.0	2.7	1.6	1.6	1.1	65.0	75.0	77.5	86.7	86.7	90.8
R5	25500	0.607	1.6	4.4	1.4	1.0	0.9	0.4	0.3	0.2	68.2	77.3	79.5	90.9	93.2	95.5
$\Phi_{T,n}$				39.5	14.9	10.6	9.8	4.7	6.3	4.0	62.4	73.0	75.3	88.1	84.1	90.0

69 ^a Projected E_x-E_m area; ^b Fractional projected area per region.

70

Table S4 Elemental composition of the Mn-based catalyst.

Element	Content proportion (wt.%)
Al	61.0
O	36.0
Mn	2.0
Ce	1.0

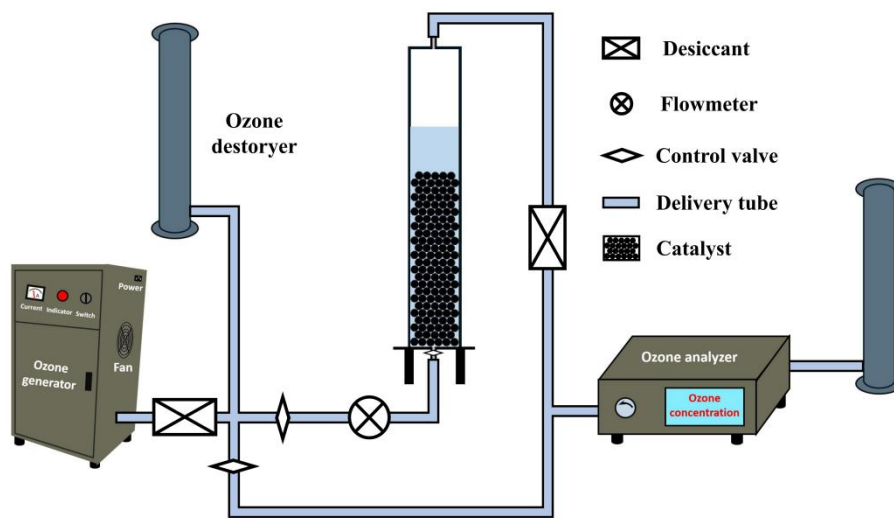


Fig. S1 Simplified diagram of the catalytic ozonation device.

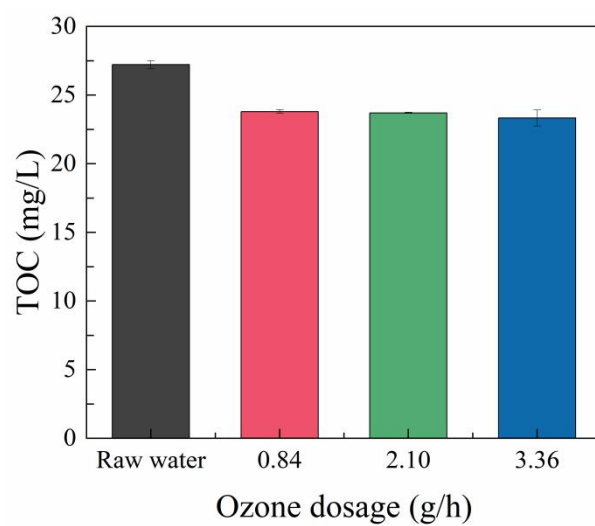


Fig. S2 Influence of ozone dosage on the TOC removal in secondary effluent from IPWWTPs in the ozonation alone process (pH = 4.0, $t=25$ °C).

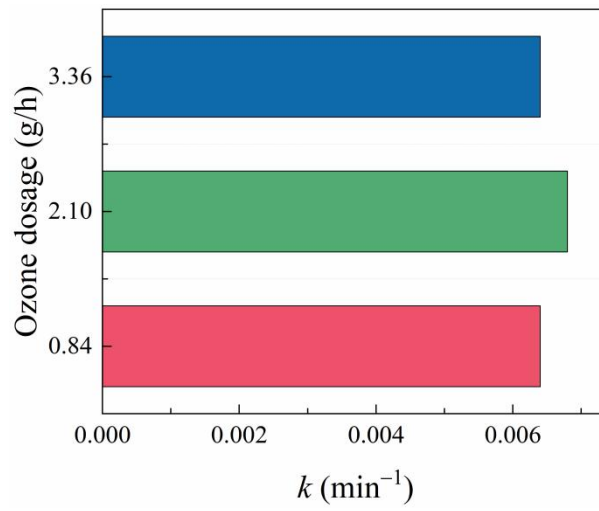


Fig. S3 Influence of ozone dosage on the initial reaction rate (k) for COD removal in secondary effluent from IPWWTPs in the ozonation alone process ($\text{pH} = 4.0$, $t = 25\text{ }^\circ\text{C}$).

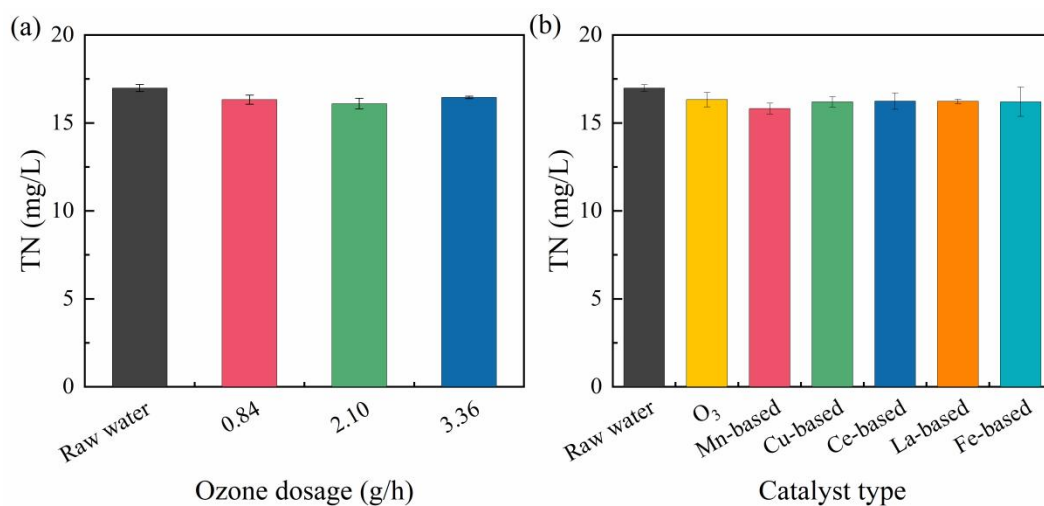


Fig. S4 Influence of ozone dosage on TN removal in secondary effluent from IPWWTPs in the ozonation process (a). (pH = 4.0, $t = 25$ °C). Influence of different catalyst on TN removal in secondary effluent from IPWWTPs in the catalytic ozonation process (b). ($[O_3] = 0.84$ g/h, $[Catalyst] = 100$ g/L, pH = 4.0, $t = 25$ °C).

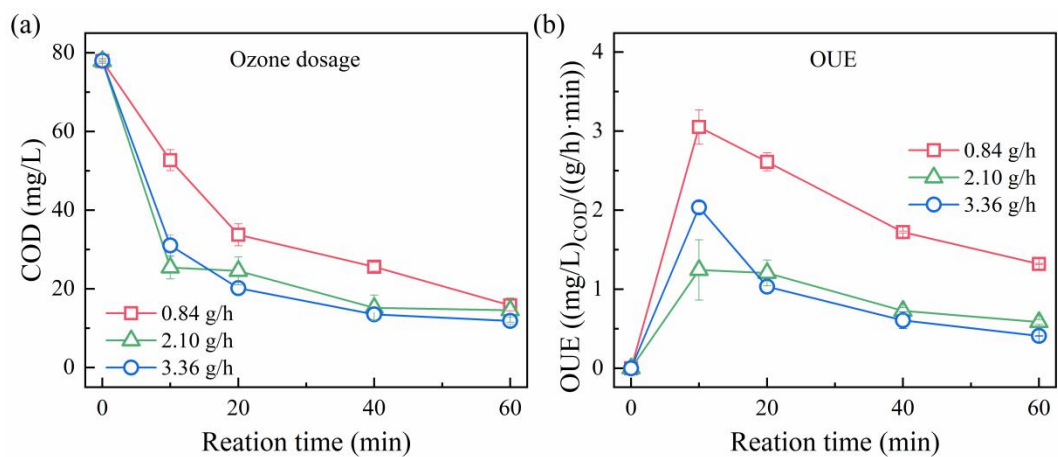


Fig. S5 Impacts of ozone dosage on the COD removal (a) and ozone utilization efficiency (b) in the Mn-based catalytic ozonation process. ([Catalyst] = 100 g/L, pH = 4.0, $t = 25$ °C).

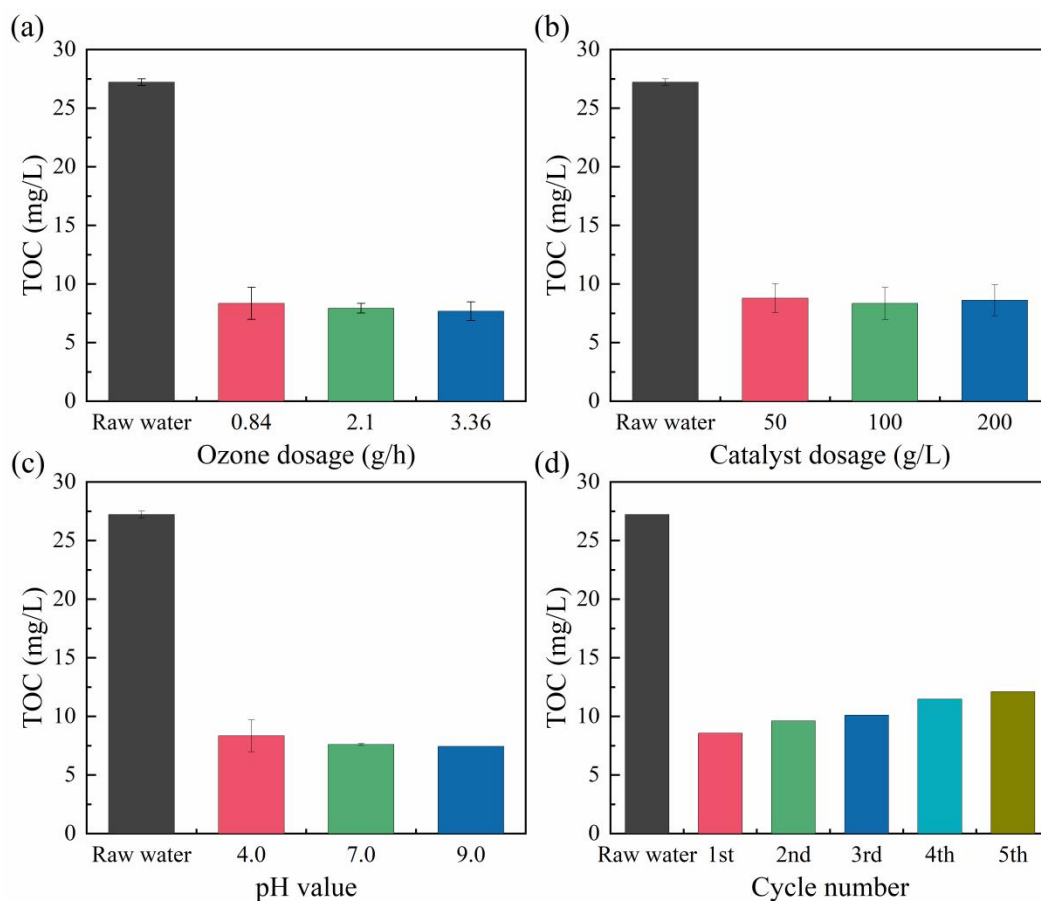


Fig. S6 Impacts of operating conditions on the TOC removal in secondary effluent from IPWWTPs in the Mn-based catalytic ozonation process. Ozone dosage (a). ($[\text{Catalyst}] = 100 \text{ g/L}$, $\text{pH} = 4.0$, $t = 25 \text{ }^\circ\text{C}$). Catalyst dosage (b). ($[\text{O}_3] = 0.84 \text{ g/h}$, $\text{pH} = 4.0$, $t = 25 \text{ }^\circ\text{C}$). pH value (c). ($[\text{O}_3] = 0.84 \text{ g/h}$, $[\text{Catalyst}] = 100 \text{ g/L}$, $t = 25 \text{ }^\circ\text{C}$). Catalyst cycle times (d). ($[\text{O}_3] = 0.84 \text{ g/h}$, $[\text{Catalyst}] = 100 \text{ g/L}$, $\text{pH} = 4.0$, $t = 25 \text{ }^\circ\text{C}$).

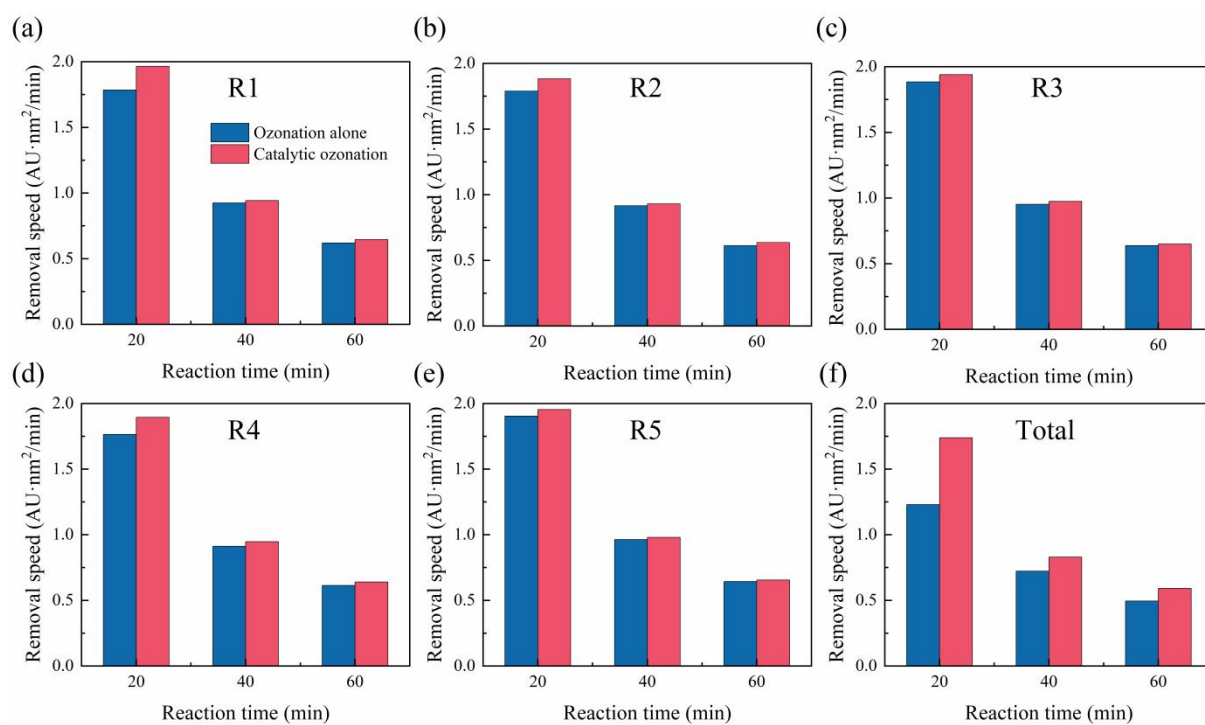


Fig. S7 FOMs removal speed during the ozonation reaction. Ozonation alone process. ($[O_3] = 0.84$ g/h, pH = 4.0, $t = 25$ °C). Catalytic ozonation process. ($[O_3] = 0.84$ g/h, [Catalyst] = 100 g/L, pH = 4.0, $t = 25$ °C).

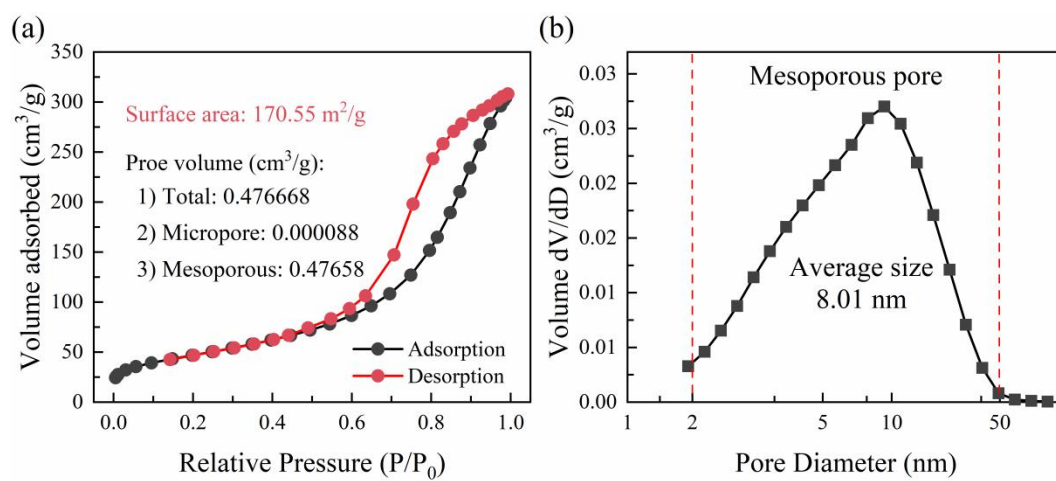


Fig. S8 N₂ adsorption-desorption isotherms (a) and pore distribution (b) of Mn-based catalyst.

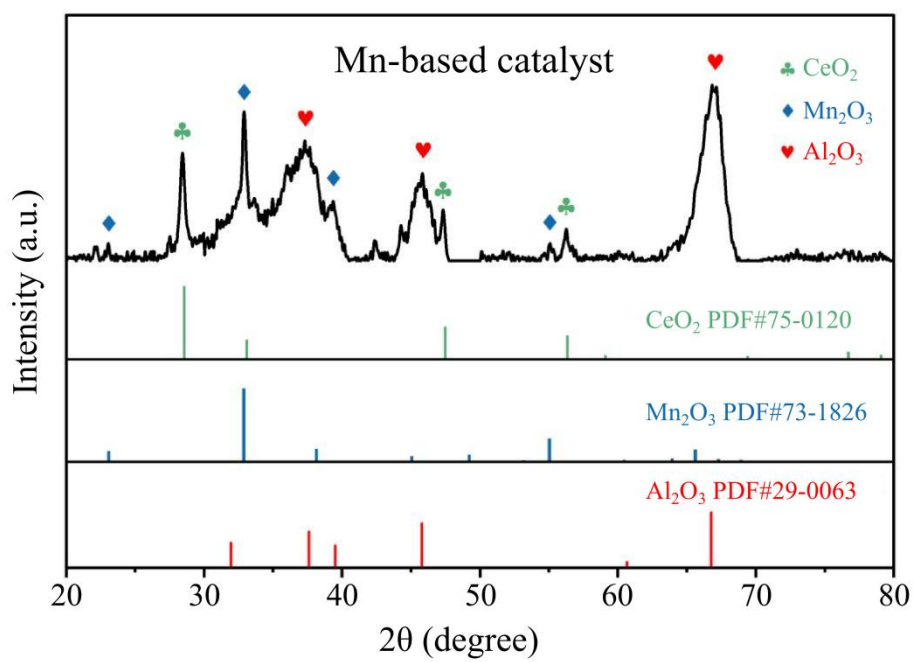


Fig. S9 XRD patterns of Mn-based catalyst.

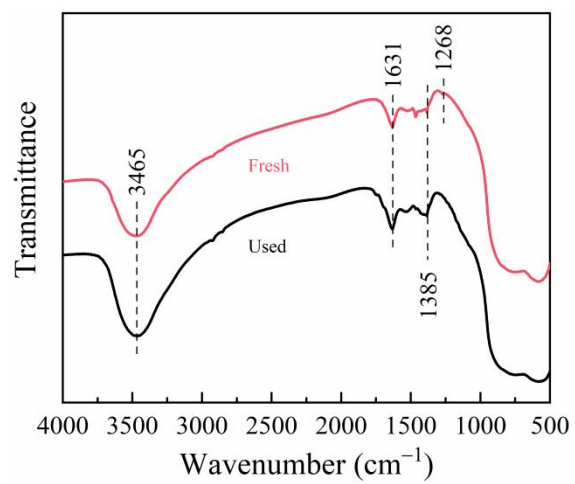


Fig. S10 FTIR spectra of the fresh and used Mn-based catalysts.

References

- Chen W, Westerhoff P, Leenheer J, Booksh K (2003) Fluorescence excitation-emission matrix regional integration to quantify spectra for dissolved organic matter. *Environment Science Technology* 37: 5701-5710.
- Yao J, Zhang Y, Dong Z K (2021). Enhanced degradation of contaminants of emerging concern by electrochemically activated peroxymonosulfate: Performance, mechanism, and influencing factors. *Chemical Engineering Journal*, 415, 128938.
- Peng J, Yin R, Yang X, Shang C (2022) A novel UVA/ClO₂ advanced oxidation process for the degradation of micropollutants in water. *Environment Science Technology* 56: 1257-1266.